© 2017. Published by The Company of Biologists Ltd | Journal of Experimental Biology (2017) 220, 2047-2056 doi:10.1242/jeb.153718

RESEARCH ARTICLE

Extreme polarisation sensitivity in the retina of the corn borer moth *Ostrinia*

Gregor Belušič[1,*], Katja Šporar[1,2] and Andrej Meglič[1]

ABSTRACT

The visual system of the European corn borer (*Ostrinia nubilalis*) was analysed with microscopy and electrophysiological methods (electroretinograms and single-cell recordings). *Ostrinia nubilalis* has a pair of mainly ultraviolet-sensitive ocelli and a pair of compound eyes, maximally sensitive to green light. The ommatidia contain a tiered, fused rhabdom, consisting of the rhabdomeres of 9–12 photoreceptor cells with sensitivity peak wavelengths at 356, 413, 480 and 530 nm. The photoreceptors in a large dorsal rim area have straight rhabdomeres and high polarisation sensitivity ($PS_{1,2}$=3.4, 14). Elsewhere, in the main retina, the majority of photoreceptors have non-aligned microvilli and negligible PS, but each ommatidium contains one or two blue-sensitive distal photoreceptors with straight microvilli parallel to the dorsoventral axis, yielding extremely high PS ($PS_{1,2,3}$=56, 63, 316). Rhabdoms containing distal cells with potentially high PS have evolved at least twice: in moths (Crambidae, Noctuidae, Saturniidae), as well as in dung beetles (Scarabaeidae). The distal photoreceptors with high PS, sensitive to vertically polarised light, represent a monopolatic system, which is unsuitable for the proper analysis of electric field vector (e-vector) orientation. However, the distal photoreceptors might be used in conjunction with polarisation-insensitive photoreceptors to detect objects that reflect polarised light with stereotyped orientation.

KEY WORDS: Moth retina, Spectral sensitivity, Polarisation sensitivity, Compound eye, Intracellular recording, Photoreceptors

INTRODUCTION

The European corn borer, *Ostrinia nubilalis* (Hübner) (Lepidoptera: Crambidae), is a nocturnal moth and an important crop pest, usually monitored with pheromones and black-light traps (Bartels et al., 1997). Unfortunately, the mechanism of attraction of insects to light sources is poorly understood, and ultraviolet (UV) light non-specifically attracts many nocturnal insects. To gain insight into the physiological basis for the visually driven behaviour of *O. nubilalis*, we studied the spectral and polarisation sensitivity (PS) of *O. nubilalis*.

Moths have sophisticated compound eyes with superposition optics (Exner, 1891; Kunze, 1969) and often a pair of ocelli (Dickens and Eaton, 1973; Dow and Eaton, 1976). Their eyes are able to convey well-resolved images (Horridge et al., 1977, 1983) and process colour even in very dim light (Kelber and Henique, 1999; Kelber et al., 2002, 2003). Moth colour vision is generally mediated by the basic components of the insect retina with UV-, blue- and green-sensitive photoreceptors (Schwemer and Paulsen, 1973; Bennett et al., 1997; Telles et al., 2014), in some cases expanded with a long-wavelength, red-sensitive spectral class (Langer et al., 1979). Moth retinae can be regionalised, with the short-wavelength and long-wavelength receptors enriched dorsally and ventrally, respectively (White et al., 2003). Additionally, the moth retina contains an extensive dorsal rim area (DRA) (Meinecke, 1981; Anton-Erxleben and Langer, 1988; White et al., 2003), i.e. an assembly of polarisation-sensitive ommatidia that assist in navigation by the polarised pattern of skylight (Labhart and Meyer, 2002).

Moth ommatidia contain nine or more photoreceptor cells, forming a fused rhabdom with their rhabdomeres (Langer et al., 1979; Schlecht, 1979). The rhabdoms are optically isolated from each other by an enveloping tracheolar tapetum, and the rhabdom layer is separated from the dioptrical apparatus by a clear zone (Land and Nilsson, 2012). Distinct photoreceptor cells contribute their rhabdomeric microvilli in different layers, thus forming a tiered rhabdom (Langer et al., 1979; Schlecht, 1979). Occasionally, thin distal parts of the rhabdom extend into the clear zone (Fischer and Horstmann, 1971; Horridge et al., 1977).

The probability of light absorption by the microvilli is highest when their long axis coincides with the direction of the electric field vector (e-vector) of incident light, and hence the PS of a photoreceptor can be inferred from the geometry of its rhabdomere (Meinecke and Langer, 1982; Wernet et al., 2012). In the main retina (i.e. outside of the DRA), the cross-section of a moth rhabdom resembles a flower, because the photoreceptors project their microvilli in different directions, often in a fan-like pattern (Fischer and Horstmann, 1971; Meinecke, 1981). Consequently, such photoreceptors have low PS. In the DRA, however, the rhabdoms appear rectangular (Langer et al., 1979). There, the photoreceptors have highly aligned, straight microvilli with potentially high PS. The different DRA photoreceptors of a rhabdom occur in two classes with orthogonally arranged microvilli, forming crossed, polarisation-opponent pairs that can analyse the e-vector of incident light independent of its intensity (Labhart, 1988). Interestingly, the ommatidia in the main retina of certain moth species contain one or two distal photoreceptors with perfectly aligned, straight microvilli (Meinecke, 1981; Anton-Erxleben and Langer, 1988), oriented in the dorsoventral direction (Anton-Erxleben and Langer, 1988), which are presumably strongly polarisation sensitive. Indeed, illumination of moth eyes with intense, polarised UV (or blue) light selectively destroyed those microvilli that were oriented in parallel with the light's e-vector, demonstrating that the distal cells were UV (or blue) sensitive, most probably with high PS (Meinecke and Langer, 1982).

Here, we present an anatomical and electrophysiological analysis of the retina of *O. nubilalis*, which reveals the properties of the retinal substrate for wavelength discrimination and the detection of polarised light. We demonstrate that *O. nubilalis* has ocelli with two spectral peaks, four spectral classes of retinal photoreceptors and two distinct sets of photoreceptors for the detection of polarised

[1]Department of Biology, Biotechnical Faculty, University of Ljubljana, SI-1000 Ljubljana, Slovenia. [2]European Neuroscience Institute, D-37077 Goettingen, Germany.

*Author for correspondence (Gregor.belusic@bf.uni-lj.si)

Received 22 November 2016; Accepted 16 March 2017

Journal of Experimental Biology (2017) 220, 2047-2056 doi:10.1242/jeb.153718

light: one in the DRA, where the rhabdomeres form orthogonal analyser pairs; and one in the main retina, where the rhabdomeres with high PS occur in a single, dorsoventral orientation.

MATERIALS AND METHODS

Animals

Experiments were performed in one European (*O. nubilalis*) and two Asian (*Ostrinia scapulalis* and *Ostrinia furnacalis*) species of corn borer. *Ostrinia nubilalis* was reared at the Slovenian Institute for Hop Research and Brewing, at the Plant Protection Institute of the Centre for Agricultural Research of the Hungarian Academy of Sciences, or caught in the western region of Slovenia. *Ostrinia scapulalis* and *O. furnacalis* were kindly donated by Professor Yukio Ishikawa, University of Tokyo. Prior to the experiments, the moths were kept in a 12 h:12 h day:night cycle at 22°C. The experiments were performed during the daytime.

Macrophotography

A whole moth was fixed with beeswax to a micromanipulator and imaged with a USB digital microscope Dino-Lite Edge AM4515ZT (AnMo Electronics, New Taipei City, Taiwan). A sequence of images was acquired at different focal planes and merged into a stack with extended depth of field in Adobe® Photoshop® CS5 (Adobe Systems Inc., San Jose, CA, USA).

Histology

Eyes were isolated from hemi-sectioned heads using a razor blade and micro-scissors. The preparation was performed under visible light, so that the eyes were light adapted.

For light microscopy (LM), complete eyes were fixated for 3 h in 3.5% glutaraldehyde and 4% paraformaldehyde in 0.1 mol l^{-1} Na-cacodylate buffer (pH 7.2). Post-fixation followed for 90 min at room temperature in 1% OsO_4 in 0.1 mol l^{-1} Na-cacodylate. The specimens were rinsed with distilled water, dehydrated in a graded ethanol series (50–100% in 10% steps) and embedded in Spurr resin (Sigma EM0300, Sigma-Aldrich, St Louis, MO, USA). Semi-thin sections were mounted on glass slides, stained with Azure II (Sigma-Aldrich) and observed with an AxioImager Z1 microscope (Zeiss, Oberkochen, Germany). Samples for transmission electron microscopy (TEM) were prepared similarly, but with the following differences: fixation in 3.5% glutaraldehyde and 4% paraformaldehyde lasted 90 min, samples were dehydrated in a graded acetone series, and Epon resin was used instead of Spurr resin. Silver ultra-thin sections were cut with a diamond knife (Histo 45, Diatome, Nidau, Switzerland), contrasted with 0.7% uranyl acetate in water for 20 min and with 2.5% lead citrate in water for 10 min, and observed with an H-7650 transmission electron microscope (Hitachi, Tokyo, Japan).

For scanning electron microscopy, the head of a female corn borer moth was enclosed in a small vial with a drop of 2% OsO_4 for 24 h, air-dried, glued with silver colloid paint to the specimen stub and sputtered with platinum in a SCD 050 Sputter Coater (Bal-Tec, Balzers, Liechtenstein). The specimen was examined in a field emission scanning electron microscope (FESEM) 7500 F (JEOL, Tokyo, Japan). The images were used to count the facets and measure their diameter.

Microspectrophotometry

Absorbance spectra of single pigment granules were measured in 1 µm-thick, fixed retinal slices. The microspectrophotometer was an AvaSpec 2048-2 CCD detector array spectrometer (Avantes, Apeldoorn, The Netherlands), mounted on a modified Leitz Ortholux microscope (Leitz, Wetzlar, Germany). A xenon arc lamp was used as a light source. The microscope objective was a LUCPlanFL N ×20/0.45 (Olympus, Tokyo, Japan).

Electrophysiological recordings

The electrophysiological experiments were performed at room temperature. The animals were immobilised with a mixture of beeswax and resin to a plastic pipette tip and pre-oriented in a miniature goniometer, mounted on a fully rotatable goniometric and xyz stage. The position of the eye with respect to the stimulus light beam was adjusted to yield maximal light responses. A 50 µm Ag/AgCl wire, inserted into the base of an antenna, served as the reference electrode.

Microelectrodes were pulled from borosilicate and quartz glass capillaries (1 mm/0.5 mm outer/inner diameter) on a P-97 Flaming/Brown or P-2000 laser Micropipette Puller (Sutter, Novato, CA, USA), and mounted on a piezo-driven micromanipulator (Sensapex, Oulu, Finland). For electroretinogram (ERG) recordings microelectrodes with an ∼1–5 µm tip, filled with insect saline (0.67% NaCl, 0.015% KCl, 0.012% $CaCl_2$, 0.015% $NaHCO_3$, pH 7.2), were driven directly through the cornea or through the cuticle next to an ocellus. For single-cell recordings, fine-tipped electrodes backfilled with 3 mol l^{-1} KCl were inserted into the eye via a small triangular hole in the cornea, which was sealed with silicon vacuum grease to prevent drying. Only young and fully hydrated animals with a minimal cut in the cornea could be used in the experiments. In older and desiccated moths, the low turgor of the clear zone caused an immediate collapse of the retina upon cutting. The electrode excursion was designed so that the photoreceptor cells were impaled perpendicular to their optical axes at the proximal end of the clear zone, ca. 200 µm below the cornea. A shallower excursion resulted in unstable recordings from the thin distal photoreceptor processes, and a deeper excursion resulted in breaking the microelectrode tip upon contacting the tracheolar sheath. Successful intracellular recordings were obtained mostly with quartz microelectrodes with a resistance of 120–250 MΩ. A retina typically yielded between zero and four stably impaled photoreceptors. The signal was amplified with a SEC 10 LX amplifier (Npi electronic, Tamm, Germany), conditioned with a Cyber Amp 320 (Axon Instruments, Union City, CA, USA) and digitised with a Micro 1401 (CED, Cambridge, UK) analog–digital (A/D) converter. The signal was low-pass filtered with an 8-pole Bessel filter to prevent aliasing and sampled at 2.5 kHz. WinWCP (Strathclyde Electrophysiology Software, Version 4.0.5) and Prism 6.0 (GraphPad, La Jolla, CA, USA) software was used for data acquisition and further analysis.

Optical set-up

The light stimulation set-up consisted of a 150 W XBO lamp, a quartz condenser and lenses, an SH05/M shutter (Thorlabs, Dachau, Germany), a monochromator (B&M Optik, Limburg, Germany) with a bandpass (FWHM) of 10 nm, a series of reflective neutral density filters on fused silica substrate (CVI Melles Griot, Didam, The Netherlands), a rotatable, continuously variable neutral-density filter on fused silica substrate NDC-100C-4 (Thorlabs), and a focusable objective stage, equipped with field and aperture diaphragms (Qioptiq, Goettingen, Germany) to control the aperture of the stimulating beam to a half-width between 1.5 deg and 15 deg. The light output was calibrated using a linear thermopile sensor (Newport Oriel, Irvine, CA, USA) and a radiometrically calibrated Flame spectrophotometer (Ocean Optics, Dunedin, FL, USA). At the level of the preparation, the maximal light flux at

Journal of Experimental Biology

Journal of Experimental Biology (2017) 220, 2047-2056 doi:10.1242/jeb.153718

467 nm was 1.5×10^{15} photons cm^2 s^{-1}. The monochromator and rotatable filter were operated with a Due microcontroller (Arduino, Italy), allowing stimuli to be produced with equal photon flux between 300 nm and 700 nm. To achieve equal photon flux, the light had to be attenuated by up to 10^{-1}. For selective chromatic adaptation, monochromatic light from an identical parallel pathway was projected to the eye coaxially with the main stimulating beam. Adapting light was attenuated with discrete neutral density filters to create approximately equal photon fluxes (±25%) at all adapting wavelengths. The eye was adapted for ∼3 min and spectral sensitivity was measured as in a dark-adapted eye.

The degree of polarisation of the stimulating set-up was checked by projecting the monochromatic light to an OPT-101 photodiode (Texas Instruments, Dallas, TX, USA) through one or two UV-capable polarising foils OUV2500 (Knight Optical, Harrietsham, UK). Stray light from the monochromator was blocked with Techspec OD 4 bandpass filters (Edmund Optics, York, UK; bandpass 50 nm, centre wavelengths 360, 450, 525 and 600 nm). The light shutter was opened and the polariser was rotated by 360 deg, yielding a sinusoidally fluctuating voltage signal at the photodiode output. The minimal and maximal photodiode voltage (V_{min}, V_{max}, respectively) within a polariser cycle was measured and the degree of polarisation (DOP) was calculated:

$$\mathrm{DOP} = (V_{max} - V_{min})/(V_{max} + V_{min}). \quad (1)$$

The stimulating light from the monochromator was intrinsically slightly polarised (DOP=1.3–4.5%; Fig. S1). The polarising foil produced highly polarised light at all tested wavelengths (DOP approaching 100%; Fig. S1).

Spectral sensitivity was measured following a few minutes of dark adaptation by applying a series of 200 ms attenuated isoquantal light pulses at 300–700 nm and 700–300 nm in 5 nm steps with sufficiently long (2–10 s) inter-stimulus intervals to avoid light adaptation. Single cells were stimulated with the beam at minimal aperture to minimise the ERG artefact. The intensity–response relationship was measured at the wavelength that yielded a maximal response, using graded light pulses ranging from −4 to 0 log intensity. For the proximal photoreceptors, the stimulus had to be additionally attenuated with 1–3 log ND filters. The stimulus–response relationship was estimated by fitting the response amplitudes $V(I)$ to the Hill (Naka–Rushton) function:

$$V(I) = V_0 I^n (R^n + I^n)^{-1}, \quad (2)$$

where I is the light intensity, V_0 is the maximal response, R is the intensity needed for a half-maximal response and n is the slope of the sigmoid. The intensity $I_c(\lambda)$ necessary to create a criterion response V_c with a monochromatic light stimulus with wavelength λ is then:

$$I_c(\lambda) = R[V_0/V_c - 1]^{-1/n}. \quad (3)$$

The spectral sensitivity was calculated as the normalised inverse criterion intensity.

PS was measured by projecting the monochromatic light pulses through a UV-capable polariser foil OUV2500 (Knight Optical). The polariser was rotated around its axis at 5.6 deg or 11.25 deg steps. Horizontally oriented e-vector was defined as 0 deg and 180 deg and vertically as 90 deg and 270 deg. Measurements were obtained at the peak wavelength of the spectral sensitivity. Light flashes that resulted in 25–75% of the maximal response amplitude were used. PS was calculated by transforming the response voltages into sensitivity using Eqn (3), and fitting the sensitivity values with a $\cos^2$ function:

$$S(\alpha) = A[\cos(\alpha + \phi)]^2 + C, \quad (4)$$

where S is the sensitivity, α is the e-vector angle, A is the amplitude, ϕ is the phase shift and C is the offset. PS was then calculated as the ratio between the sensitivity maximum and minimum, i.e. $PS=S_{max}/S_{min}$.

RESULTS

Anatomy

The visual system of *O. nubilalis* is composed of a pair of ocelli and a pair of compound eyes with superposition optics (Fig. 1). The diameter of the compound eyes of female *O. nubilalis* is ca. 1.5 mm. Males have slightly larger eyes, but as we found no differences between the ultrastructure and physiological properties of the male and female retina, all results from both sexes were merged. Each eye is composed of ca. 3000 ommatidia with facet diameter 15 µm (Fig. 1B,C), consisting of (from distal to proximal) the dioptrical apparatus consisting of corneal lenses with surface nipples (Fig. 1D) and an elongated crystalline cone, the clear zone with pigment cells containing pigment granules and the retina made up of the sets of photoreceptors (Fig. 2A–C). In the clear zone of each ommatidium, the processes of the photoreceptors form a distal rhabdom with ∼2 µm diameter (Fig. 2C1). The rhabdomeres of 9–12 retinula cells form the proximal rhabdom (Fig. 2C2). A small,

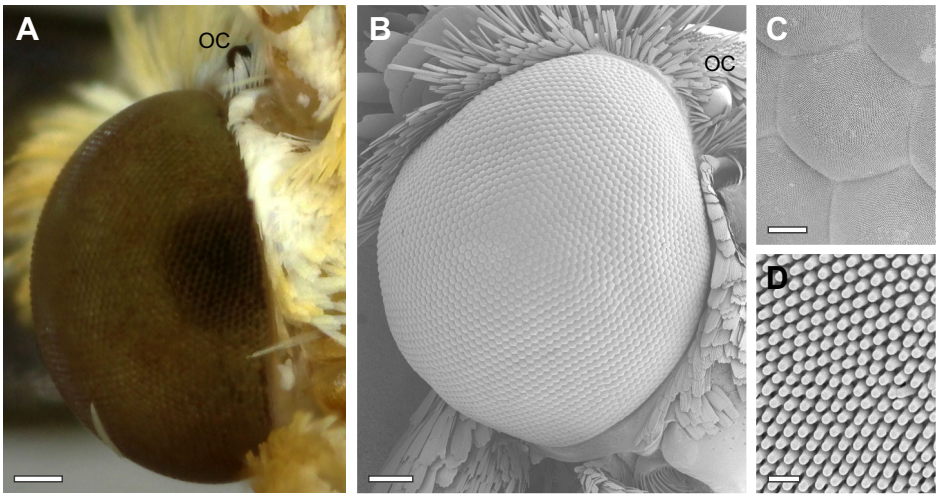

Fig. 1. External appearance of the visual system. (A) Macrophotograph of the head of a female European corn borer moth (frontal view). (B–D) Scanning electron micrographs. (B) Overview of the right half of the head with a compound eye and an ocellus (OC). (C) Facet lenses. (D) Corneal surface nipples (nipple diameter ca. 120 nm). Scale bars: A and B, 100 µm; C, 5 µm; D, 0.5 µm.

Journal of Experimental Biology (2017) 220, 2047-2056 doi:10.1242/jeb.153718

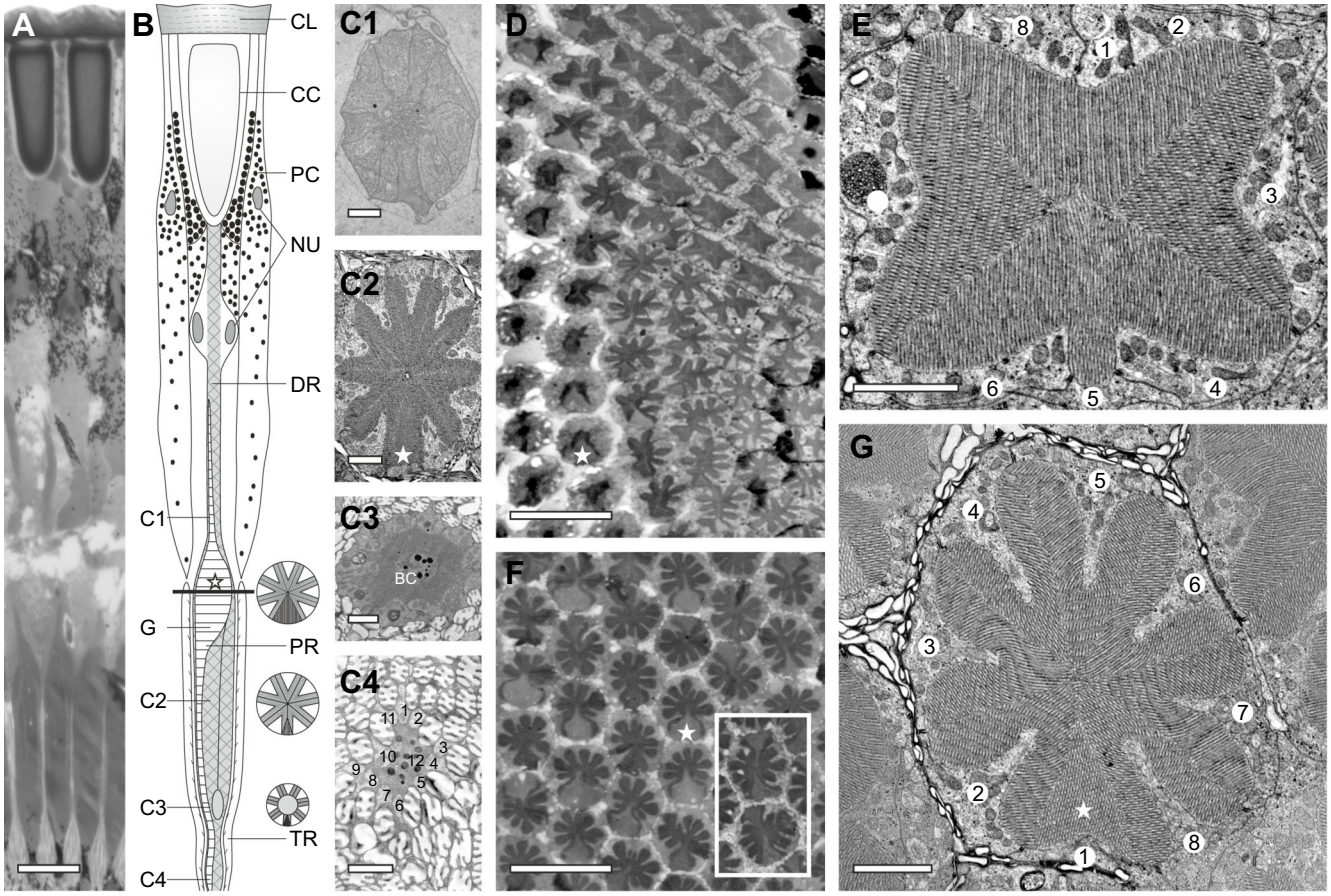

Fig. 2. Anatomy of the retina of *Ostrinia nubilalis*. (A,D,F) Light micrographs. (C,E,G) Transmission electron micrographs. (A) Longitudinal section of the retina. (B) Schematic drawing of the ommatidium in A; the dioptrical apparatus in the distal part consists of a corneal lens (CL) and a crystalline cone (CC); the central part is the clear zone with the secondary pigment cells (PC), photoreceptor and PC nuclei (NU), and the distal rhabdom (DR); the proximal part contains the proximal rhabdom (PR) and the tracheoles (TR), which form a tapetum. The circles on the right represent the schematic drawings of the rhabdom cross-section at the three levels. (C) Cross-sections at four depths are indicated by the sublabels C1–C4 on the left in B. (C1) Distal rhabdom in the clear zone. (C2) Proximal rhabdom in the main retina. (C3) Rhabdom proximal to the tapetum. The basal cell (BC) is very small and pigmented. (C4) The tapetum, formed by ribbed tracheolar tubes, penetrated by the axons of the 12 enumerated photoreceptors of an ommatidium. (D) Cross-section of the central and dorsal retina; most of the retina is occupied by the flower-shaped rhabdoms (lower half); the dorsal part (upper half) is occupied by a large dorsal rim area with rectangular rhabdoms. (E) Cross-section of a rhabdom in the dorsal rim area. (F) Cross-section of the main retina at the distal level of the proximal rhabdom, indicated by the horizontal line in B; at this level, most ommatidia contain a large distal photoreceptor cell, characterised by the light staining (indicated by an asterisk in B, D, F and G). Inset in F, rhabdoms containing two lightly stained distal photoreceptors. (G) Cross-section of a rhabdom in the main retina, slightly proximally to the section in F; the distal photoreceptor cell (1) is somewhat thinner than the other photoreceptors. Scale bars: A, D and F, 20 µm; C1–C4, E and G, 2 µm.

pigmented basal photoreceptor cell (Fig. 2C3) is apposed to the tracheolar tapetum, which optically isolates the rhabdoms and creates a mirror at the proximal part of the retina (Fig. 2C4).

The compound eye has an extensive DRA, consisting of ∼100 ommatidia, as inferred from the semi-thin sections. The rhabdom cross-section has a rectangular to slightly cushion-like shape (Fig. 2D,E). Each rhabdom in the DRA is formed by orthogonally positioned rhabdomeres (Fig. 2E). The microvilli of each rhabdomere are aligned in one direction along the entire photoreceptor depth, thus forming an excellent anatomical substrate for the detection of linearly polarised light.

Ommatidia in the rest of the retina (‘the main retina’) have a flower-shaped rhabdom cross-section (Fig. 2D,F,G). Here, most of the photoreceptor cell bodies have a triangular profile, and their microvilli are arranged approximately perpendicular to the longer sides of the triangle. Hence, the microvilli of a single cell subtend all angles between 0 deg and 90 deg (Fig. 2G). Such an arrangement of the microvilli effectively minimises the PS of a photoreceptor. However, in the transition zone between the clear zone and the main rhabdom layer (Fig. 2B, horizontal line), most of the rhabdom cross-section is occupied by the distal photoreceptor cell with an enlarged rhabdomere in the shape of a droplet. In semi-thin sections, stained with Azure, the rhabdomeres of these photoreceptors appear lighter than the rhabdomeres of adjacent photoreceptors (Fig. 2F, asterisk in F,G). The rhabdomeres of the distal photoreceptors taper towards proximally and there occupy only a small fraction of rhabdom (Fig. 2C2). The microvilli of the distal photoreceptors are aligned along the dorsoventral axis of the retina along the entire depth of the photoreceptor, and the distal photoreceptor is therefore potentially the only cell type in the main retina that is sensitive to the direction of the e-vector of linearly polarised light.

Microelectrode recordings

We characterised the visual organs of *O. nubilalis* by recording from the eyes and ocelli. We first recorded from the ocelli and the retina of 10 animals using extracellular electrodes to determine the spectral sensitivity via electroretinography. The ERG spectral sensitivity of dark-adapted ocelli has a large peak in the UV at ∼360 nm and a

Journal of Experimental Biology (2017) 220, 2047-2056 doi:10.1242/jeb.153718

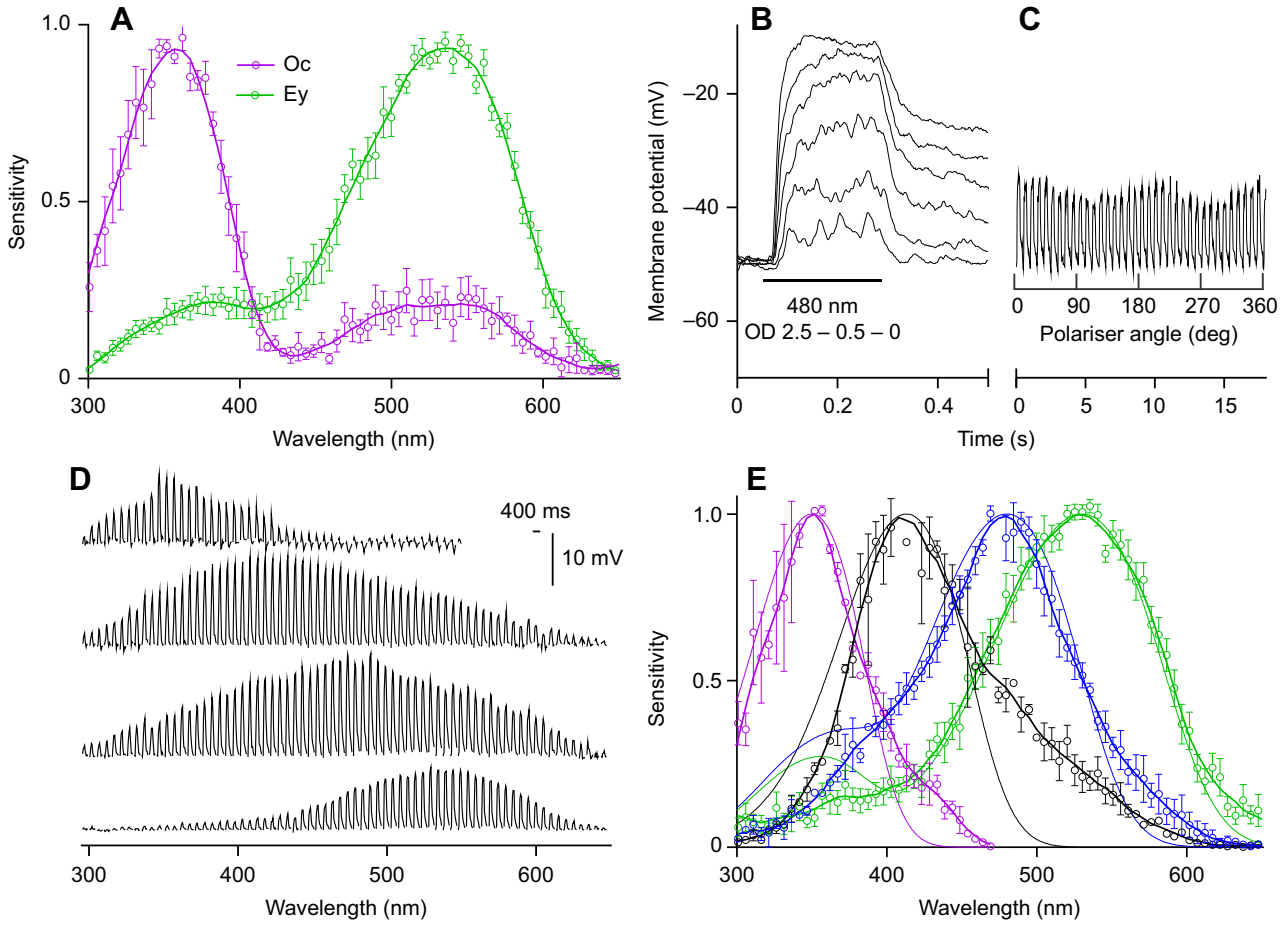

Fig. 3. Spectral sensitivity of *Ostrinia nubilalis*. (A) Spectral sensitivity (electroretinography; mean±s.e.m.) of the compound eyes (Ey) (λ_{max}=536 nm; green; *N*=7) and ocelli (Oc) (λ_{max}=358 nm; violet; *N*=5). (B) Intracellularly recorded responses of a blue-sensitive photoreceptor to 200 ms/480 nm light flashes, graded in 0.5 log intensity steps (OD, optical density of the ND filter). (C) Responses of the cell in B to 200 ms/480 nm light flashes, presented through a rotating polariser. (D) Intracellularly recorded responses to isoquantal spectral stimulus sequences of (from top to bottom) an ultraviolet (UV)-, a violet-, a blue- and a green-sensitive photoreceptor. (E) Spectral sensitivity (intracellular recordings, mean±s.e.m.) of the four photoreceptor classes, peaking at 352 nm (violet; *N*=2), 413 nm (black; *N*=2), 480 nm (blue; *N*=4) and 530 nm (green; *N*=15); thin curves are rhodopsin nomograms with peaks at the same wavelengths. Thick curves in A and E represent smoothed data with adjacent averaging of three data points.

smaller peak in the green at ∼520 nm (Fig. 3A). Using chromatic adaptation, we could only slightly suppress the sensitivity of the ocelli in the green or UV part of the spectrum.

Quite differently, the ERG spectral sensitivity of the dark-adapted retina has a small peak in the UV at ∼380 nm and a large peak in the green at ∼530 nm (Fig. 3A). Chromatic adaptation at any wavelength always caused a non-specific fall in sensitivity below 500 nm (Fig. S2A) due to the movement of short-wavelength absorbing screening pigment granules into the light path (Fig. S2B). We systematically recorded from the different regions in the retina (ventral, equatorial, dorsal, DRA), which yielded virtually identical ERG spectral sensitivities of the different eye parts in both sexes.

We performed intracellular photoreceptor recordings using sharp microelectrodes in 30 moths. The photoreceptor cells could be impaled at the proximal end of the clear zone, ca. 200 µm from the cornea, just before the electrode tip was broken by the tracheoles. The receptor potentials were relatively slow (response latency minimally 11–16 ms; no fast adaptation at high light intensity) and noisy due to photon shot noise (Fig. 3B). In most preparations, we could obtain one or two quality cells, which allowed the recording of their response to the intensity series, as well as to the polarisation and spectral scan (Fig. 3B–D). Consistent with the ERG recordings, the spectral sensitivity of most cells in the main retina was maximal in the green (Fig. 3E, green curve; λ_{max}=530 nm; *N*=15; 20 more cells not included in the analysis). Additionally, we encountered cells maximally sensitive in the blue (blue curve, λ_{max}=480 nm; *N*=4), violet (black curve, λ_{max}=413 nm; *N*=2) and UV (violet curve, λ_{max}=352 nm; *N*=2). The different photoreceptor classes were encountered stochastically. In the dorsal part of the retina, adjacent to the ocellum, we successively impaled several photoreceptors with high but not extreme PS, before hitting the head capsule. Two of these photoreceptors, which were most likely a part of the DRA, had sensitivity maxima at 480 nm and 530 nm, respectively (spectral sensitivity data merged with the blue- and green-sensitive cells from the main retina). The continuous sensitivity curves were obtained by smoothing the spectral sensitivity data by adjacent averaging of three data points (Fig. 3E). For comparison, we plotted the theoretical rhodopsin absorbance curves (Stavenga, 2010), calculated with fixed parameters (α-peak, λ_{max}=352 nm, 413 nm, 480 nm and 530 nm; β-peak, amplitude 0.25, λ_{max}=350 nm).

We measured the PS of each impaled photoreceptor at its sensitivity peak wavelength. In the main retina, all green-, UV- and violet-sensitive cells and one blue-sensitive cell (signals in Fig. 3B,C) had very low polarisation sensitivities (PS≈1–1.1).

Journal of Experimental Biology (2017) 220, 2047-2056 doi:10.1242/jeb.153718

However, we encountered three blue-sensitive photoreceptor cells (λ_{max}=480 nm) with extreme sensitivity to the direction of the e-vector (Fig. 4A). All three cells ceased to respond to light flashes when the polariser was oriented horizontally (i.e. perpendicular to the dorsoventral axis of the retina). The PS curve strongly deviated from a $\cos^2$-function and resembled an all-or-none function with additional peaks due to receptor adaptation (Fig. 4A,B). The zero response to horizontally polarised light yielded an infinite PS value. A conservative estimate of the minimal PS could be obtained by calculating the inverse value of the transmittance of the neutral density filter at which the photoreceptor ceased to respond to unpolarised test flashes in the intensity run, yielding $PS_{1,2,3}$=316, 63, 56. The only candidate cells for the polarisation-sensitive photoreceptors

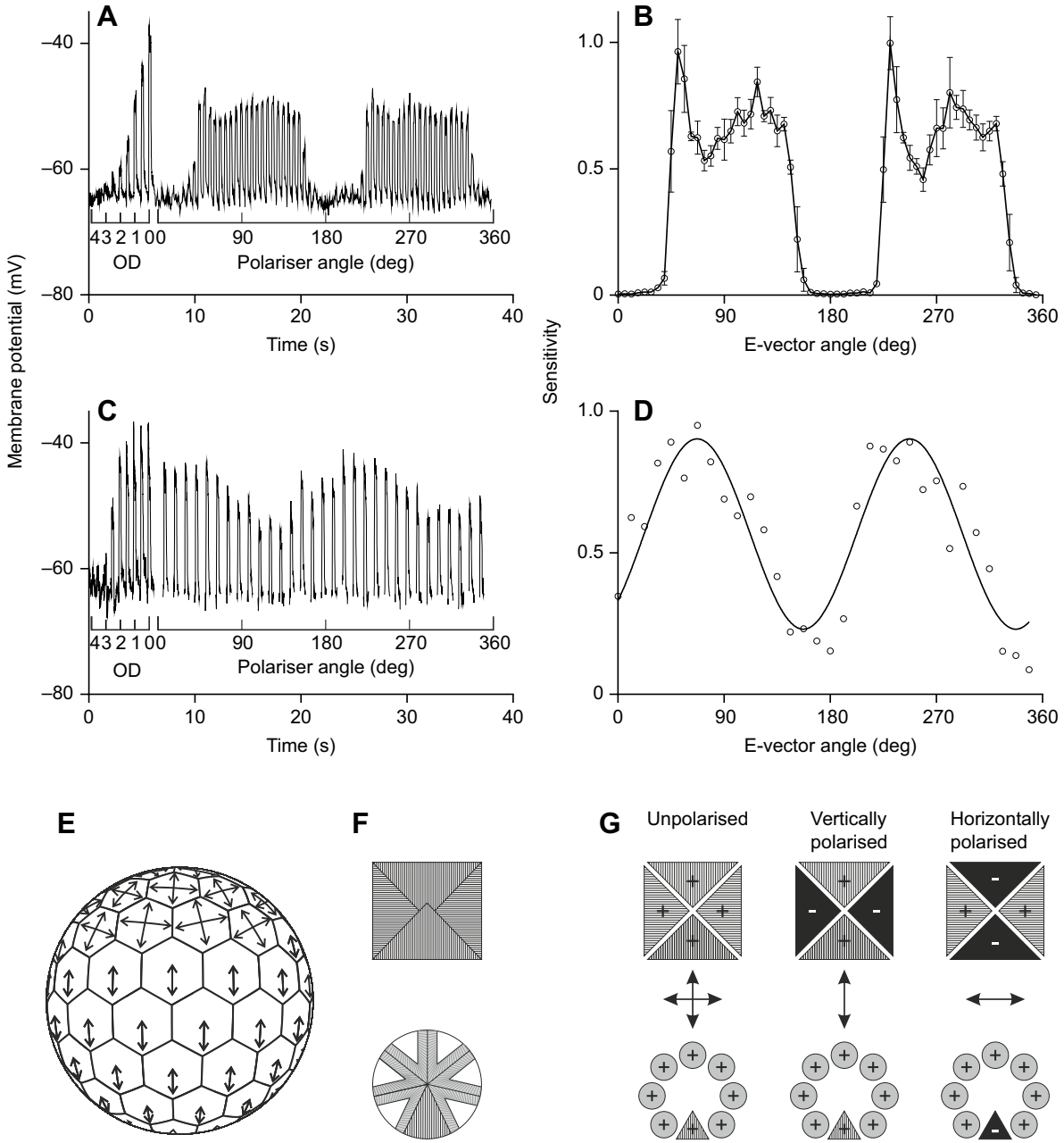

Fig. 4. Polarisation sensitivity of photoreceptors from the main retina (A,B) and the dorsal rim area (C,D) in *Ostrinia nubilalis*. (A,C) Intracellularly recorded responses of polarisation-sensitive photoreceptors from the main retina (A) and from the dorsal rim area (DRA) (C) to light flashes at 480 nm, graded in 0.5 log intensity steps, and to a sequence of 480 nm flashes (vertical bars below the voltage traces), presented through a rotating polariser (0 deg is horizontal). (B) Polarisation sensitivity of the photoreceptor from A (mean±s.e.m.; mean of four consecutive experiments in the same cell). (D) Polarisation sensitivity of the photoreceptor from C, fitted with a $\cos^2$-function. (E) Substrate for polarisation vision in the different parts of the eye; ventral and central retina contain an array of distal photoreceptors (vertical arrows), sensitive to vertically polarised light; the DRA contains rectangular rhabdoms with orthogonally positioned, polarisation-sensitive photoreceptors (crossed arrows). (F) Schematic representation of the rhabdom in the DRA (top) and the main retina (bottom); the wide distal cell has aligned microvilli. (G) Patterns of excitation in DRA rhabdom (top row) and in the main rhabdom (bottom row) upon the detection of unpolarised (left column), vertically (middle column) and horizontally (right column) polarised light. Note that the main rhabdom only creates a specific signal in the latter case. OD, optical density.

Journal of Experimental Biology

Journal of Experimental Biology (2017) 220, 2047-2056 doi:10.1242/jeb.153718

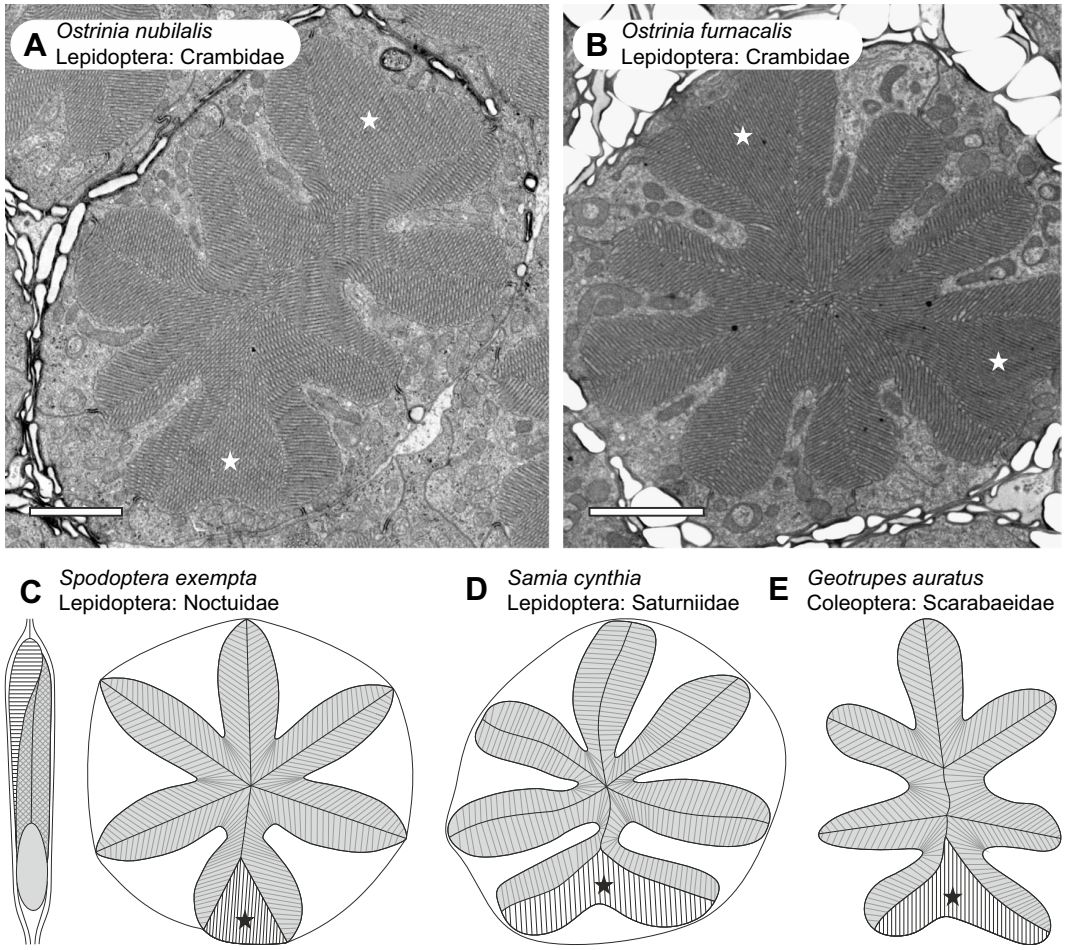

Fig. 5. Substrate for polarisation sensitivity outside of the dorsal rim area. (A) European corn borer. (B) Asian corn borer. A and B show examples of rhabdom with two distal photoreceptors, encircled by the orthogonally oriented microvilli of adjacent photoreceptors. (C) African armyworm moth (redrawn from Langer et al., 1979). (D) Silk moth (redrawn from Eguchi and Horikoshi, 1984). (E) Dung beetle (redrawn from Gokan, 1989). Asterisks indicate the photoreceptors with aligned microvilli. Scale bars: A and B, 2 µm.

in the main retina are the distal photoreceptors with straight microvilli (Figs 2F,G and 5A,B).

The blue and green photoreceptors, most likely located in the DRA, showed classical sinusoidal polarisation sensitivities, with PS_{blue}=14 and PS_{green}=3.4 (Fig. 4C,D). Our results thus show that the retina of *O. nubilalis* is populated by two separate sets of polarisation-sensitive photoreceptors; those in the DRA have orthogonally aligned microvilli, with rather high PS, and the distal photoreceptors in the main retina have dorsoventrally aligned microvilli, with extremely high PS (Fig. 4E,F).

DISCUSSION

Our study represents the first detailed electrophysiological investigation of the spectral and PS of moth photoreceptors, supported by anatomical data. Intracellular recordings from moth photoreceptors are well known to be technically very challenging, and this prevented us from marking the recorded cells with intracellular dyes. So far, the spectral sensitivity of moth photoreceptors has been inferred from microspectrophotometry of extracts of visual pigments (Schwemer and Paulsen, 1973; Langer et al., 1986), anatomical preparations (Langer et al., 1979, 1986), and extracellular recordings (Höglund et al., 1973; Horridge et al., 1977; Schlecht, 1979; Crook et al., 2014; Telles et al., 2014). Intracellular recordings have remained very rare (Horridge et al., 1983; White et al., 1983). We have to emphasise here that single-cell recordings are crucial in colour vision studies because the spectral sensitivity of a photoreceptor often substantially differs from its rhodopsin absorption spectrum. A photoreceptor's spectral sensitivity can be modified by screening pigments acting as optical filters (Arikawa et al., 1999a,b; Wakakuwa et al., 2004), by lateral filtering in the fused rhabdom (Snyder et al., 1973) and by electrical interactions of the different photoreceptors (Matić, 1983). A combination of these effects may have caused the modifications of the spectral sensitivities of the UV-, violet- and blue-sensitive photoreceptors. Their experimentally measured spectral sensitivities around the peaks are slightly narrower than the corresponding 356 nm, 413 nm and 480 nm nomograms (Fig. 3E, thin curves), indicating that the sensitivity is sharpened by the filtering by the adjacent rhabdoms with different rhodopsins. At longer wavelengths, however, these receptors show unusually high sensitivity, possibly due to electrical coupling with the long-wavelength photoreceptors, co-expression of other opsins, or high transmittance of screening pigments. The green-sensitive photoreceptors have a slightly broader sensitivity peak than that of the 530 nm nomogram. These photoreceptors probably occur in multiple copies per ommatidium, which reduces the sharpening of their spectral sensitivity via lateral filtering by other spectral classes. Their β-peak in the UV is probably reduced by the lateral filtering by

Journal of Experimental Biology (2017) 220, 2047-2056 doi:10.1242/jeb.153718

the other receptor classes and by the screening pigments that absorb mostly in the short-wavelength part of the spectrum.

The retina of *O. nubilalis* codes the light spectrum between 300 nm and 650 nm with four evenly spaced spectral classes of photoreceptors (the distance between adjacent peaks of spectral sensitivity is $\Delta\lambda_{max}$=50–80 nm). A fifth photoreceptor class, possibly sensitive to very long wavelengths, in the form of the basal receptor might have evaded our study, being inaccessible to the microelectrode due to the tracheolar sheath. However, compared with the red-sensitive, large basal cell of the moth *Spodoptera* (Langer et al., 1979), the basal cell in *O. nubilalis* is very small (Fig. 2C3), and it therefore seems to have little physiological importance except in very bright light. The potential for tetrachromatic vision by the four receptor classes in the retina of *O. nubilalis* is supplemented by the putatively dichromatic ocelli. Having now revealed the spectral richness of the visual system of *O. nubilalis*, this may open new possibilities for the development of more specific and effective light traps.

The presented data strongly suggest that the retina of *O. nubilalis* is equipped with a double substrate for polarisation vision. The presence of a large DRA with orthogonal analysers indicates that navigating *O. nubilalis* could be assisted with polarisation vision, based on the detection of e-vectors in the sky, although skylight navigation has not yet been demonstrated in any moth species. The DRA rhabdoms, arranged in a fan-like pattern, most likely reside at the input to the neurons with receptive fields that match the patterns of skylight e-vector, as is the case in locusts (Bech et al., 2014).

The polarisation-sensitive distal cells outside the DRA occur in singlets, without any obvious opponent polarisation-sensitive cells with orthogonal microvilli. Thus, they represent a monopolatic system, which in itself cannot analyse the e-vector orientation (Labhart, 2016). However, their high spatial order and extremely high PS suggest that they do participate in a distinct, novel submodality of polarisation vision. The putative downstream PS visual interneurons that compare the signals from photoreceptors with common field of view, however, will receive signals from quasi-opponent pairs, formed by the distal, polarisation-sensitive versus the proximal, polarisation-insensitive photoreceptors. To understand the neural image created by the monopolatic and the dipolatic systems in the main retina and the DRA, respectively, we presented two simplified ommatidia (Fig. 4G). The one in the DRA was composed of an orthogonal analyser pair whereas the one in the main retina was composed of one distal and seven proximal photoreceptors. Illumination creates specific patterns of receptor excitation, indicated with + and – for high and small depolarisation, respectively. The schematised ommatidia are presented with three extreme scenarios: the photoreceptors look into a bright 'white' object reflecting unpolarised light, vertically polarised light or horizontally polarised light. Unpolarised bright light will strongly excite all photoreceptors in both parts of the retina (Fig. 4G, left column). Vertically polarised light (Fig. 4G, middle column) will excite only two photoreceptors with vertical microvilli in the DRA, but all photoreceptors in the main retina, including the distal photoreceptor. Therefore, the ommatidium in the main retina cannot allow the neurons to discriminate unpolarised and vertically polarised bright light. Horizontally polarised light (Fig. 4G, right column) will excite two photoreceptors in the DRA, and all proximal, but not the distal, photoreceptors in the main retina. Thus, in the main retina, horizontally polarised light will create a specific pattern of photoreceptor excitation different from that created by unpolarised light. However, due to the low absolute sensitivity of the distal photoreceptor, low-intensity, unpolarised light will create a similar excitation pattern, indistinguishable from the pattern created by horizontally polarised light. In order for the monopolatic system to specifically detect horizontally polarised light, an additional thresholding mechanism should be employed in the putative neuropil, operated by the absolute level of excitation of the proximal photoreceptors. Thus, a bright polarised patch, such as a reflection from a leaf surface or water, could be resolved from a dim patch with a similar spectral composition. Alternatively, the distal photoreceptors might feed into a system for the 'successive mode' of polarisation vision (Kirschfeld, 1972). A polarised object will evoke a strongly fluctuating signal in the distal receptors, if observed from different angles during locomotion.

Within the genus *Ostrinia*, the ommatidia contain one or two distal photoreceptors (Fig. 2F, inset, Fig. 5A,B), and the retinal anatomy appears to be highly conserved as can be inferred from the TEM sections in *O. furnacalis* (Fig. 5B) and from the LM sections of other moths in the family Crambidae (Lau et al., 2007). Anatomically similar distal photoreceptors exist also in other families of moths, such as the owlet moths (Meinecke, 1981) (Noctuidae, Fig. 5C), the silk moths (Eguchi and Horikoshi, 1984; Anton-Erxleben and Langer, 1988) (Saturniidae, Fig. 5D) and possibly also in the snout moths (Fischer and Horstmann, 1971) (Pyralidae). Strikingly, a similar rhabdom organisation might have independently evolved in Coleoptera with superposition eyes, such as the dung beetles (Gokan, 1989) (Scarabaeidae, Fig. 5E). Polarisation vision outside the DRA has been also demonstrated in the apposition eyes of the butterfly *Papilio* (Kelber et al., 2001; Kinoshita et al., 2011), backswimmer bugs, dragonflies and locusts to detect water (Schwind, 1983, 1985; Wildermuth, 1998; Shashar et al., 2005), in horseflies to detect mammalian fur (Horvath et al., 2008), and in fruit flies (Wernet et al., 2012).

The extraordinary physiological properties of the distal photoreceptor raise many questions. Here, we described it as a blue-sensitive cell, but it is likely that a minor subpopulation of UV-sensitive distal receptors exists in the retina of *O. nubilalis*, similarly as in *Spodoptera* (Meinecke and Langer, 1984). The distal receptors probably do not contribute to colour vision, because high PS prevents reliable wavelength discrimination (Wehner and Bernard, 1993; Kelber et al., 2001). We propose that they are tuned to short wavelengths to optimally match the spectral composition of skylight, reflected from shiny surfaces as polarised light. Their PS exceeds the highest values ever measured in any arthropod species (e.g. PS>21 in the DRA of the bee *Megalopta*) (Greiner et al., 2007; review in Stowasser and Buschbeck, 2012), except for the case of the fly DRA cells R7marg and R8marg, which produce hyperpolarising responses to polarised stimuli in the non-preferred direction (Hardie, 1984; Weir et al., 2016). In the fly DRA, the high PS is, however, possible due to filtering in a tiered rhabdom and electrical interactions between the two photoreceptors in a polarisation-opponent pair (Weir et al., 2016). How then is such high PS achieved in a moth's cell, which has no orthogonally positioned opponent photoreceptors? Perfectly aligned rhodopsin molecules in a microvillus yield a highest dichroic ratio Δ_M=20 and consequently a similar magnitude of the PS=20 in a thin photoreceptor slice with negligible self-screening (Snyder and Laughlin, 1975). In *Ostrinia*, PS above this limit is possible because of the selective absorption of light that is polarised in the non-preferred direction by the microvilli of adjacent photoreceptors (Fig. 5A,B). Furthermore, the possibly detrimental effects of self-screening on PS (Snyder, 1973) in the distal photoreceptor are reduced by its favourable geometry. Its rhabdomere occupies a large

Journal of Experimental Biology

cross-sectional area only at a very shallow, distal-most part of the rhabdom, and then quickly tapers down to a very small wedge. Thus, the distal photoreceptor is equivalent to a thin slice of aligned microvilli. Additionally, self-screening might also be reduced by the low density of rhodopsin molecules. In the semi-thin sections, the rhabdomere of the distal photoreceptor was always stained very lightly (Fig. 2D,F), perhaps due to the low protein content, and we were never able to saturate its responses even with the brightest flashes (Fig. 4A, intensity run). Lastly, absorption of polarised light by the distal photoreceptor must be very low as it does not seem to substantially polarise light absorbed by the proximal photoreceptors, which have negligible PS. Minimal self-screening is associated with low photon yield and is certainly not well suited for low light conditions. The polarisation-sensitive distal photoreceptors could only have evolved in compound eyes with a large entrance pupil, i.e. in eyes with superposition optics. We suggest that they are used to visually recognise the horizontally polarised reflections from water bodies or foliage, or vertically polarised skylight pattern in the north and south at sunset or sunrise. Finally, the array of polarisation detectors in the main retina could also operate in concert with the DRA, and support navigation in difficult conditions.

Acknowledgements
The authors thank Drs Kentaro Arikawa and Kazimir Drašlar for their assistance with electron microscopy, Dr Doekele Stavenga for commenting on the manuscript and assistance in microspectrophotometry, and Drs Magda Rak Cizej, Yukio Ishikawa and Gabriella Köblös for the moths.

Competing interests
The authors declare no competing or financial interests.

Author contributions
Conceptualisation: G.B. Methodology: G.B., K.Š., A.M. Validation: G.B. Formal analysis: G.B., K.Š., A.M. Investigation: G.B. Data curation: G.B., K.Š., A.M. Writing – original draft: G.B., A.M. Writing – review & editing: G.B., K.Š., A.M. Visualisation: G.B., K.Š., A.M. Supervision: G.B. Project administration: G.B. Funding acquisition: G.B.

Funding
The study was funded by the Air Force Office of Scientific Research European Office of Aerospace Research and Development (grant FA9550-15-1-0068 to G.B. and A.M.), ARRS (grant P3-0333 to G.B.) and by the Slovene-Japan bilateral project of the Slovene research agency (ARRS) (BI-JP/13-15-003).

Supplementary information
Supplementary information available online at
http://jeb.biologists.org/lookup/doi/10.1242/jeb.153718.supplemental

References
Anton-Erxleben, F. and Langer, H. (1988). Functional morphology of the ommatidia in the compound eye of the moth, *Antheraea polyphemus* (Insecta, Saturniidae). *Cell Tissue Res.* **252**, 385-396.
Arikawa, K., Mizuno, S., Scholten, D. G. W., Kinoshita, M., Seki, T., Kitamoto, J. and Stavenga, D. G. (1999a). An ultraviolet absorbing pigment causes a narrow-band violet receptor and a single-peaked green receptor in the eye of the butterfly *Papilio*. *Vision Res.* **39**, 1-8.
Arikawa, K., Scholten, D. G. W., Kinoshita, M. and Stavenga, D. G. (1999b). Tuning of photoreceptor spectral sensitivities by red and yellow pigments in the butterfly *Papilio xuthus*. *Zool. Sci.* **16**, 17-24.
Bartels, D. W., Hutchison, W. D. and Udayagiri, S. (1997). Pheromone trap monitoring of Z-strain European corn borer (Lepidoptera: Pyralidae): optimum pheromone blend, comparison with blacklight traps, and trap number requirements. *J. Econ. Entomol.* **90**, 449-457.
Bech, M., Homberg, U. and Pfeiffer, K. (2014). Receptive fields of locust brain neurons are matched to polarization patterns of the sky. *Curr. Biol.* **24**, 2124-2129.
Bennett, R. R., White, R. H. and Meadows, J. (1997). Regional specialization in the eye of the sphingid moth *Manduca sexta*: blue sensitivity of the ventral retina. *Visual Neurosci.* **14**, 523-526.
Crook, D. J., Hull-Sanders, H. M., Hibbard, E. L. and Mastro, V. C. (2014). A comparison of electrophysiologically determined spectral responses in six subspecies of *Lymantria*. *J. Econ. Entomol.* **107**, 667-674.
Dickens, J. C. and Eaton, J. L. (1973). External ocelli in Lepidoptera previously considered to be anocellate. *Nature* **242**, 205-206.
Dow, M. A. and Eaton, J. L. (1976). Fine-structure of ocellus of cabbage-looper moth (*Trichoplusia-ni*). *Cell Tissue Res.* **171**, 523-533.
Eguchi, E. and Horikoshi, T. (1984). Comparison of stimulus-response (V-log I) functions in five types of lepidopteran compound eyes (46 species). *J. Comp. Physiol. A* **154**, 3-12.
Exner, S. (1891). *Die Physiologie der facettierten Augen von Krebsen und Insekten*. Leipzig – Vienna: Franz Deuticke.
Fischer, A. and Horstmann, G. (1971). [Fine structure of the eye of the meal moth, *Ephestia kuehniella* Zeller (Lepidoptera, Pyralididae)]. *Z. Zellforsch. Mik. Anat.* **116**, 275-304.
Gokan, N. (1989). The compound eye of the dung beetle *Geotrupes auratus* (Coleoptera, Scarabaeidae). *Appl. Entomol. Zool.* **24**, 133-146.
Greiner, B., Cronin, T. W., Ribi, W. A., Wcislo, W. T. and Warrant, E. J. (2007). Anatomical and physiological evidence for polarisation vision in the nocturnal bee *Megalopta genalis*. *J. Comp. Physiol. A* **193**, 591-600.
Hardie, R. C. (1984). Properties of photoreceptor R7 and photoreceptor R8 in dorsal marginal ommatidia in the compound eyes of *Musca* and *Calliphora*. *J. Comp. Physiol. A* **154**, 157-165.
Höglund, G., Hamdorf, K. and Rosner, G. (1973). Trichromatic visual system in an insect and its sensitivity control by blue light. *J. Comp. Physiol. A* **86**, 265-279.
Horridge, G. A., McLean, M., Stange, G. and Lillywhite, P. G. (1977). A diurnal moth superposition eye with high resolution *Phalaenoides tristifica* (Agaristidae). *Proc. R. Soc. B* **196**, 233-250.
Horridge, G. A., Marčelja, L. and Jahnke, R. (1983). Retinula cell responses in a moth superposition eye. *Proc. R. Soc. B* **220**, 47-68.
Horváth, G., Majer, J., Horváth, L., Szivák, I. and Kriska, G. (2008). Ventral polarization vision in tabanids: horseflies and deerflies (Diptera: Tabanidae) are attracted to horizontally polarized light. *Naturwissenschaften* **95**, 1093-1100.
Kelber, A. and Henique, U. (1999). Trichromatic colour vision in the hummingbird hawkmoth, *Macroglossum stellatarum* L. *J. Comp. Physiol. A* **184**, 535-541.
Kelber, A., Thunell, C. and Arikawa, K. (2001). Polarisation-dependent colour vision in *Papilio* butterflies. *J. Exp. Biol.* **204**, 2469-2480.
Kelber, A., Balkenius, A. and Warrant, E. J. (2002). Scotopic colour vision in nocturnal hawkmoths. *Nature* **419**, 922-925.
Kelber, A., Balkenius, A. and Warrant, E. J. (2003). Colour vision in diurnal and nocturnal hawkmoths. *Integr. Comp. Biol.* **43**, 571-579.
Kinoshita, M., Yamazato, K. and Arikawa, K. (2011). Polarization-based brightness discrimination in the foraging butterfly, *Papilio xuthus*. *Philos. Trans. R. Soc. B Biol. Sci.* **366**, 688-696.
Kirschfeld, K. (1972). Notizen: Die notwendige Anzahl von Rezeptoren zur Bestimmung der Richtung des elektrischen Vektors linear polarisierten Lichtes. *Z. Naturforsch.* **27**, 578-579.
Kunze, P. (1969). Eye glow in the moth and superposition theory. *Nature* **223**, 1172-1174.
Labhart, T. (1988). Polarization-opponent interneurons in the insect visual system. *Nature* **331**, 435-437.
Labhart, T. (2016). Can invertebrates see the e-vector of polarization as a separate modality of light? *J. Exp. Biol.* **219**, 3844-3856.
Labhart, T. and Meyer, E. P. (2002). Neural mechanisms in insect navigation: polarization compass and odometer. *Curr. Opin. Neurobiol.* **12**, 707-714.
Land, M. F. and Nilsson, D.-E. (2012). *Animal Eyes*. Oxford Animal Biology Series. New York: Oxford University Press Inc.
Langer, H., Hamann, B. and Meinecke, C. C. (1979). Tetrachromatic visual system in the moth *Spodoptera exempta* (Insecta: Noctuidae). *J. Comp. Physiol. A* **129**, 235-239.
Langer, H., Schmeinck, G. and Anton-Erxleben, F. (1986). Identification and localization of visual pigments in the retina of the moth, *Antheraea polyphemus* (Insecta, Saturniidae). *Cell Tissue Res.* **245**, 81-89.
Lau, T. F. S., Gross, E. M. and Meyer-Rochow, V. B. (2007). Sexual dimorphism and light/dark adaptation in the compound eyes of male and female *Acentria ephemerella* (Lepidoptera: Pyraloidea: Crambidae). *Eur. J. Entomol.* **104**, 459-470.
Matić, T. (1983). Electrical inhibition in the retina of the butterfly *Papilio*. *J. Comp. Physiol. A* **152**, 169-182.
Meinecke, C. C. (1981). The fine structure of the compound eye of the African armyworm moth, *Spodoptera exempta* Walk. (Lepidoptera, Noctuidae). *Cell Tissue Res.* **216**, 333-347.
Meinecke, C.-C. and Langer, H. (1982). Structural reactions to polarized light of microvilli in photoreceptor cells of the moth *Spodoptera*. *Cell Tissue Res.* **226**, 225-229.

Meinecke, C.-C. and Langer, H. (1984). Localization of visual pigments within rhabdoms of the compound eye of *Spodoptera exempta* (Insecta, Noctuidae). *Cell Tissue Res.* **238**, 359-368.
Schlecht, P. (1979). Colour discrimination in dim light: An analysis of the photoreceptor arrangement in the moth *Deilephila*. *J. Comp. Physiol. A* **129**, 257-267.
Schwemer, J. and Paulsen, R. (1973). Three visual pigments in *Deilephila elpenor* (Lepidoptera, Sphingidae). *J. Comp. Physiol. A* **86**, 215-229.
Schwind, R. (1983). A polarization-sensitive response of the flying water bug *Notonecta glauca* to UV Light. *J. Comp. Physiol. A* **150**, 87-91.
Schwind, R. (1985). A further proof of polarization vision of *Notonecta glauca* and a note on threshold intensity for eliciting the plunge reaction. *Experientia* **41**, 466-467.
Shashar, N., Sabbah, S. and Aharoni, N. (2005). Migrating locusts can detect polarized reflections to avoid flying over the sea. *Biol. Lett.* **1**, 472-475.
Snyder, A. W. (1973). Polarization sensitivity of individual retinula cells. *J. Comp. Physiol. A* **83**, 331-360.
Snyder, A. W. and Laughlin, S. B. (1975). Dichroism and absorption by photoreceptors. *J. Comp. Physiol. A* **100**, 101-116.
Snyder, A. W., Menzel, R. and Laughlin, S. B. (1973). Structure and function of the fused rhabdom. *J. Comp. Physiol. A* **87**, 99-135.
Stavenga, D. G. (2010). On visual pigment templates and the spectral shape of invertebrate rhodopsins and metarhodopsins. *J. Comp. Physiol. A* **196**, 869-878.
Stowasser, A. and Buschbeck, E. K. (2012). Electrophysiological evidence for polarization sensitivity in the camera-type eyes of the aquatic predacious insect larva *Thermonectus marmoratus*. *J. Exp. Biol.* **215**, 3577-3586.
Telles, F. J., Lind, O., Henze, M. J., Rodríguez-Gironés, M. A., Goyret, J. and Kelber, A. (2014). Out of the blue: the spectral sensitivity of hummingbird hawkmoths. *J. Comp. Physiol. A* **200**, 537-546.
Wakakuwa, M., Stavenga, D. G., Kurasawa, M. and Arikawa, K. (2004). A unique visual pigment expressed in green, red and deep-red receptors in the eye of the small white butterfly, *Pieris rapae crucivora*. *J. Exp. Biol.* **207**, 2803-2810.
Wehner, R. and Bernard, G. D. (1993). Photoreceptor twist: a solution to the false-color problem. *Proc. Natl. Acad. Sci. USA* **90**, 4132-4135.
Weir, P. T., Henze, M. J., Bleul, C., Baumann-Klausener, F., Labhart, T. and Dickinson, M. H. (2016). Anatomical reconstruction and functional imaging reveal an ordered array of skylight polarization detectors in *Drosophila*. *J. Neurosci.* **36**, 5397-5404.
Wernet, M. F., Velez, M. M., Clark, D. A., Baumann-Klausener, F., Brown, J. R., Klovstad, M., Labhart, T. and Clandinin, T. R. (2012). Genetic dissection reveals two separate retinal substrates for polarization vision in *Drosophila*. *Curr. Biol.* **22**, 12-20.
White, R. H., Brown, P. K., Hurley, A. K. and Bennett, R. R. (1983). Rhodopsins, retinula cell ultrastructure, and receptor potentials in the developing pupal eye of the moth *Manduca sexta*. *J. Comp. Physiol. A* **150**, 153-163.
White, R. H., Xu, H., Münch, T. A., Bennett, R. R. and Grable, E. A. (2003). The retina of *Manduca sexta*: rhodopsin expression, the mosaic of green-, blue- and UV-sensitive photoreceptors, and regional specialization. *J. Exp. Biol.* **206**, 3337-3348.
Wildermuth, H. (1998). Dragonflies recognize the water of rendezvous and oviposition sites by horizontally polarized light: a behavioural field test. *Naturwissenschaften* **85**, 297-302.